Available online at www.sciencedirect.com
ScienceDirect
International Journal of Pharmaceutics 340 (2007) 163–172
INTERNATIONAL JOURNAL OF PHARMACEUTICS
www.elsevier.com/locate/ijpharm

Pharmaceutical Nanotechnology

Preparation, characterization and biodistribution of the lactone form of 10-hydroxycamptothecin (HCPT)-loaded bovine serum albumin (BSA) nanoparticles

Lei Yang, Fude Cui *, Dongmei Cun, Anjin Tao, Kai Shi, Wenhui Lin

School of Pharmacy, Shenyang Pharmaceutical University, Wenhua Road 103, Shenyang City, Liaoning, China

Received 4 May 2006; received in revised form 22 January 2007; accepted 15 March 2007
Available online 25 March 2007

Abstract

10-Hydroxycamptothecin (HCPT) is insoluble in both water and physiological acceptable organic solvents and tends to change into its carboxylate form, which shows minimal anticancer activity and several unpredictable side effects. The goal of this study is to exploit an appropriate delivery system for HCPT to improve the stability of its lactone form. Bovine serum albumin (BSA) nanoparticles entrapping HCPT were prepared by reformative emulsion-heat stabilization technique. During this process, HCPT transformed from lactone to carboxylate and finally back to lactone form successfully. A simple reversed-phased HPLC method was developed to analyze both lactone and carboxylate forms of HCPT synchronously. Mean particle size and the ratio of lactone and carboxylate forms of HCPT were evaluated to investigate the effects of the formulations and preparation conditions. It was indicated the percentage of lactone form of HCPT in resultant BSA nanoparticles could be improved over 95% through adjusting the concentration of NaOH solution and the stirring time after high-speed emulsification. This drug delivery system was also characterized by dynamic light scattering (DLS) and light microscopy. The investigations on drug loading, in vitro release and body distribution in rats after intravenous (i.v.) administration were also carried out. It was found that the obtained nanoparticles showed spherical shape with the mean particle size of around 600 nm, and drug loading content, encapsulation efficiency and yield achieved 2.21%, 57.5% and 90.5% with the optimal preparation conditions, respectively. The in vitro release behavior exhibited a sustaining release manner and was affected by the trypsin in medium. HCPT could release more than 90% within 20 h in the medium of pH 7.4 PBS containing 750 U/ml trypsin, but only 25% within 40 h in the pure pH 7.4 PBS. The results of body distribution study in rats showed the liver targeting potential of HCPT–BSA nanoparticles that 59.6%, 52.9% and 55.3% of the examined amount of lactone HCPT accumulated in livers at 1, 4 and 24 h after injection, respectively. These results suggest that the HCPT–BSA nanoparticles seem to be a stable delivery system for poorly soluble HCPT or its derivatives.

Keywords: 10-Hydroxycamptothecin (HCPT); Bovine serum albumin (BSA); Nanoparticles; Lactone form; Drug delivery system

1. Introduction

Camptothecin (CPT) and related analogues are promising anticancer agents with a novel mechanism of action, targeting the nuclear enzyme topoisomerase I (Top I) and inhibiting the relegation of the cleaved DNA strand, which leads to the death of tumor cells (Jaxel et al., 1989; Rothenberg, 1997). One of the nature CPT analogues, 10-hydroxycamptothecin (HCPT), has been shown to have a strong antitumor activity against gastric carcinoma, hepatoma, leukemia, and tumor of head and neck, and, more importantly, HCPT is more potent and less toxic in experimental animals and in human clinical evaluations, mainly in China. However, due to its poor solubility in water and in physiological acceptable organic solvents, practical use of HCPT is limited. Moreover, the opening of the labile E-ring at physiological pH and above, which may render the drug much less active and highly toxic (O'Leary and Muggia, 1998), represents a bigger obstacle to the wide clinical application of CPTs. The earlier clinical trials using its highly water-soluble sodium salt, HCPT–Na^+, which was the product of opening the lactone ring of HCPT, showed minimal anticancer activity and several unpredictable side effects such as myelosuppression, hemorrhagic

* Corresponding author. Tel.: +86 23986355; fax: +86 23986355.
E-mail address: kkyanglei@hotmail.com (F. Cui).

0378-5173/$ – see front matter © 2007 Elsevier B.V. All rights reserved.
doi:10.1016/j.ijpharm.2007.03.028

cystitis, diarrhea, nausea, vomiting, and dermatitis. Therefore, it is very important to separate and quantitate the two forms of HCPT.

Compared to water-soluble CPT analogues, fewer studies have been conducted with water-insoluble HCPT, because the insolubility and instability of the drug in its active lactone form make it very difficult to devise a suitable formulation for clinical testing. A kind of poly(lactide-co-glycolide) (PLGA) microspheres was investigated to stabilize and deliver HCPT for the treatment of cancer (Shenderova et al., 1997); Lundberg (1998) prepared oleic acid esters of the CPT analogues HCPT, which could be intercalated into liposome bilayers and submicron lipid emulsions; The liver targeting and sustained release hydroxycamptothecin polybutylcyanoacrylate nanoparticles (HCPT–PBCA-NP) (Zhang and Lu, 1997), which were wrapped up with ployvinylpyrrolidone (PVP) were prepared by adsorption-enwrapping method; Zhang (Zhang et al., 2004) synthesized triblock copolymers of poly(caprolactone-co-lactide)-b-PEG-b-poly(caprolactone-co-lactide) (PCLLA–PEG–PCLLA)by ring opening copolymerization of caprolactone and lactide in the presence of poly(ethylene glycol) (PEG). With such triblock copolymers, PCLLA–PEG–PCLLA nanoparticles entrapping HCPT (Hatefi and Amsden, 2002) were prepared by nano-precipitation method. Among the many ways to solve the solubility problem associated with the delivery of water-insoluble HCPT, employing the polymeric nanoparticulate drug delivery system might be one of the simplest methods, except that the 'passive' targeting ability was not obvious.

Since bovine serum albumin (BSA) could significantly retard the CPT lactone ring opening as compared with the control (Opanasopit et al., 2005), in this paper, HCPT–BSA-NP was prepared by emulsion-heat stabilization technique, which was proved more promising in terms of formulation stability, biocompatibility and the 'passive' targeting ability. During the preparing process of HCPT–BSA-NP, HCPT transformed from lactone to carboxylate and finally back to lactone form. Moreover, we have developed the procedure to analyze both lactone and carboxylate forms of HCPT synchronously with a reversed-phased HPLC system. The influences of formulation and technique factors on particle size, drug loading, the form of HCPT and in vitro release were evaluated in some detail. Preliminary investigation on the body distribution in rats of HCPT loaded in BSA nanoparticles was also conducted. The results show that the nanoparticles possessed the 'passive' targeting ability to liver and could deliver HCPT mainly in its active lactone form.

2. Materials and methods

2.1. Materials

10-hydroxycamptothecin (HCPT, 99.2%, Junjie, China); bovine serum albumin (BSA, >98%, Yuanheng, China); span 80 (Lanxing, China); NaOH (96%, Zhengxin, China); ammonium acetate (98%, Bodi, China); trypsin (1:250, BBI). All other reagents were of analytical grade, and double distilled water was used throughout. All solutions used in HPLC analysis were of HPLC grade and filtered using a 0.45 μm membrane filter (Hi-Tech, China) with a filtration system (SHB-III, China).

2.2. Reverse-phase HPLC analysis of lactone–carboxylate ratio of HCPT

Reverse-phase HPLC system was utilized for simultaneous determination of the lactone and sodium carboxylate (HCPT–Na^+) forms of HCPT, which was improved according to reported analytical methods (Li and Zhang, 1996; Ma et al., 2002). The two forms of HCPT were separated within a single chromatographic run. Reverse-phase HPLC system for this determination consisted of a Hitachi Hyper LC-900 system (Japan) at a flow rate of 0.8 ml/min at 30 °C. For separation a DiamonsilTM reverse-phase C_{18} column (150 mm × 4.6 mm, 5 μm, Dikma, USA) was employed. The mobile phase was composed of 25% acetonitrile and 75% 0.075 M ammonium acetate buffer (pH 6.4). The detection was performed by a UV–vis absorption at 266 nm.

2.3. Preparation of standards

HCPT stock solution: HCPT was dissolved in an appropriate amount of dimethylsulfoxide (DMSO). The solutions were stored at −20 °C.

HCPT standard solutions: the stock solution was diluted with DMSO 0.01 M sodium phosphate, pH 2.5 (50/50, v/v) and DMSO 0.05 M phosphate buffer, pH 9 (50/50, v/v) for lactone and sodium carboxylate forms standard solution, respectively. The solutions were equilibrated at ambient for 30 min and stored at 4 °C. The standard solutions were used in the same day when they were prepared.

2.4. Preparation of HCPT–BSA nanoparticles

HCPT–BSA nanoparticles were prepared by reformative emulsion-heat stabilization technique. 6 mg of HCPT and 150 mg of BSA were dissolved in 0.6 ml of 0.04 mol/l NaOH solution by vortex. The aqueous solution was added to 30 ml of castor oil containing 2% Span-80 at room temperature with the stirring speed of 1200 rpm and emulsified with high-speed of 9000 rpm by a homogenizer (FA-25, Fluko, China) for 5 min, and then it was unceasingly stirred for 40 min. The resultant emulsion was added dropwise to 60 ml of castor oil at 140 ± 5 °C, which was being stirred at 1200 rpm. After the emulsion was added heating was continued for 15 min. The suspension was then allowed to cool to room temperature. Once this temperature had been reached stirring was stopped and 90 ml of petroleum ether was added to the nanoparticle–castor oil suspension. The mixture was stirred homogeneously, and then transferred to centrifuge vessels and centrifuged at 12,000 rpm for 15 min (TGL-16G, Anke, China). The supernatant was decanted and 90 ml of petroleum ether was added to the nanoparticles. The nanoparticles were resuspended in the petroleum ether using an ultrasonic water bath (KQ-100, China). This suspension was then centrifuged at 3000 rpm for 5 min. The ether

phase was decanted and this washing step was repeated two times. After decanting the final ether wash, the nanoparticles were resuspended in 6 ml of petroleum ether, and stored at 4 °C in an airtight container.

2.5. Size, zeta potential and morphology of the nanoparticles

Mean diameter and size distribution of the prepared nanoparticles were determined by dynamic light scattering (DLS) using a Coulter LS230 instrument (Beckman-Coulter Co. Ltd., USA). Zeta potential of the nanoparticles was obtained with Coulter DELSA 440SX instrument (Beckman-Coulter Co. Ltd., USA). Each sample of the nanoparticle suspension was adjusted to a concentration of 0.05% (w/v) in filtered water in the case of zeta potential examination. Both particle sizing and zeta potential measurements were triplicated for a single batch of nanoparticles and the results were the average of the three measurements.

Morphological examination of the nanoparticles was conducted using light microscope (DMBA450, Motic).

2.6. Nanoparticle yield, drug loading content and encapsulation efficiency

To determine the drug loading content, a predetermined aliquot of nanoparticle suspension was withdrawn and vacuum-dried at 40 °C, and the residue was accurately weighted before thoroughly dissolved in 0.5% trypsin–water solution. Then the equivalent volume of DMSO was added to it after 2 h. The exact HCPT concentration in the resulted water–DMSO solution was then determined by the HPLC at the wavelength of 266 nm. Then the total amount of the drug contained in the withdrawn nanoparticle suspension could be calculated. Drug loading content and encapsulation efficiency were obtained by Eqs. (1) and (2), respectively. Nanoparticle yield was determined gravimetrically by Eq. (3):

$$\text{Drug loading content (\%)} = \frac{\text{weight of the drug in nanoparticles}}{\text{weight of the nanoparticles}} \times 100 \quad (1)$$

$$\text{Encapsulation efficiency (\%)} = \frac{\text{weight of the drug in nanoparticles}}{\text{weight of the feeding drug}} \times 100 \quad (2)$$

$$\text{Nanoparticle yield (\%)} = \frac{\text{weight of the nanoparticles}}{\text{weight of the feeding polymer and drug}} \times 100 \quad (3)$$

2.7. In vitro release of HCPT loaded nanoparticles

Release of HCPT was measured using a dialysis tubing (12,000–14,000 DM-27, Millipore, USA) as previously reported (Opanasopit et al., 2004). A 100 ml phosphate buffered saline (PBS) at pH 7.4 was used as a medium at 37 ± 1 °C under constant vibrating using a constant-temperature shaker (SHA-B, Guohua, China). Appropriate amount of HCPT–BSA nanoparticles were suspended in 5 ml 750 U/ml trypsin–PBS solution. Two milliliters of these mixtures were placed in a dialysis bag and immersed in the medium. At certain time intervals, 1 ml aliquots of the medium were withdrawn, and the same volume of fresh medium was added. The sample solution was analyzed by reverse-phase HPLC after the equivalent amount of DMSO was added. All experiments were performed in triplicate.

2.8. Body distribution of HCPT loaded nanoparticles in rats

The body distribution experiment was carried out by combining the published in vivo distribution methods of HCPT–PCLLA–PEG–PCLLA nanoparticles (Zhang et al., 2004) and terbutaline sulfate loaded albumin microspheres (Sahin et al., 2002). The rats, body weight between 150 and 170 g (provided by Central Animal Laboratory of Shenyang Pharmaceutical University, China), were used for body distribution investigations. They were fasted overnight but had free access to water and about 2 ml suspension of HCPT loaded nanoparticles (corresponding to 5 mg HCPT/kg) was injected intravenously into the tail vein. 1, 4 and 24 h were chosen as sampling points and three rats were i.v. injected with HCPT loaded nanoparticles for each sampling point. At the predetermined time, the animals were dissected and each tested organ was collected. Organ samples were washed and accurately weighed, and stored at −20 °C till analysis. During the body distribution study, the concentration of HCPT was assayed by HPLC method mentioned above.

The tissues were homogenized and extracted with four volumes of 0.5% trypsin–water/DMSO (1:1). Then it was centrifuged at 15,000 rpm for 5 min and 20 μl of the clear supernatant was injected into the HPLC system. The concentrations of HCPT in all samples were determined based on the peak area comparing with the reference which was prepared by adding certain amount of HCPT–DMSO solution to extraction solution of vacant tissues.

3. Results and discussion

3.1. Separation of lactone and carboxylate forms of HCPT

In this test, if pH is in the range of 5.0–7.5, the mobile phase will influence little on the transformation between two forms of HCPT (Fassberg and Stella, 1992). Therefore, 0.075 M ammonium acetate buffer (pH 6.4)-acetonitrile (75:25) was selected as the mobile phase. The method developed in the present study meets the needs of simultaneous determination of lactone and carboxylate forms of HCPT. A representative chromatogram of the two forms of HCPT is shown in Fig. 1. In the Fig. 1C, standard lactone and carboxylate forms of HCPT were mixed prior to injection. The retention times of carboxylate and lactone HCPT are 3.2 and 9.4 min.

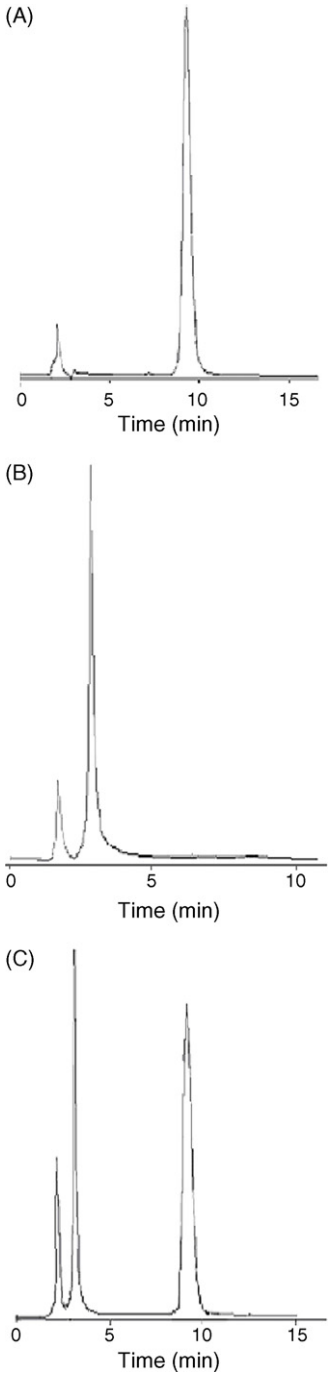

Fig. 1. Chromatograms of standard solutions: (A) lactone form of HCPT; (B) carboxylate form of HCPT (HCPT–Na^+); (C) a mixture of lactone and carboxylate forms of HCPT.

3.2. Preparation and characterization of HCPT–BSA nanoparticles

In the preliminary experiment, several methods were attempted to prepare HCPT–BSA nanoparticles, however, compared with emulsion-heat stabilization technique various disadvantages were produced by other methods: nanoparticles prepared by emulsification-crossing method showed much lower drug loading content; polymeric dispersing method increased the particle size markedly; with regard to monophasic coagulation method, the resultant emulsion was unstable. Since HCPT was stable by heating, the emulsion-heat stabilization technique was adopted finally.

From this initial method, a number of variables were identified which might affect the final nanoparticle size. These variables were: BSA concentration, high-speed emulsification time, and aqueous-to-non-aqueous phase volume ratio. In addition to the above emulsification variables, the following variables relating to heat stabilization were evaluated: emulsion drop rate, heat stabilization temperature, and heat stabilization time.

Since particle size has a crucial impact on the in vivo fate of a particulate drug delivery system, control over the particle size is of great importance for drug carriers. Each variable was evaluated sequentially by preparing one batch of nanoparticles for each level listed in Table 1. From the particle size analysis the optimal level of each variable was determined at that level which produced the smallest diameter (Gallo et al., 1984).

As BSA concentration was the first variable studied, three batches of nanoparticles were prepared by adding 90, 150 or 210 mg BSA to 0.6 ml of NaOH solution containing 6 mg HCPT, which was employed as aqueous phase. At this point the initial method of preparation (see above) was followed. Since a BSA concentration of 250 mg/ml produced the smallest particle diameter (see Table 1), it was used for all subsequent variables studied. Therefore, to study the next variable, high-speed emulsification time, three batches of nanoparticles were prepared using 0.6 ml of NaOH solution containing 6 mg HCPT and 150 mg BSA, and high-speed emulsification time of 2, 5 or 8 min. As each new variable was studied, the initial method of nanoparticle preparation was altered in accordance with the results on the optimum level of each preceding variable. This type of experimental design ignores interactions between the variables.

It was shown in Table 1 that an increase in BSA concentration tended to produce a smaller nanoparticle. Since, the differences were minor and high concentration of BSA resulted in low drug loading (the concentration of HCPT was determined as 10 mg/ml), 250 mg/ml was considered as the optimal level to investigate subsequent variables. In our system, it was believed that, upon emulsification, the albumin at the w/o interface would unfold with the hydrophobic groups exposed to the non-aqueous medium, and the hydrophilic groups oriented towards the aqueous phase. Such a protein denaturation process will render the nanoparticles hydrophobic in nature. In this case the albumin would act as an emulsifying agent and thus its concentration might affect the droplet size and stability of the emulsion.

It was well documented that the time of emulsification and the phase volume would affect the droplet size of emulsions, and therefore, the resultant nanoparticle size (Eberth and Merry, 1983; Li and Folger, 1979). The largest effect on particle size for different emulsification times was seen in going from 2 to 5 min with the high-speed of 9000 rpm. It was felt that longer emulsification times would produce a smaller particle size, but this was not obvious while exceeding 5 min. The aqueous-to-non-aqueous phase volume ratio had a relatively large effect on the

Table 1
Mean particle diameters for BSA nanoparticles prepared under different conditions

Order of evaluation	Variable	Level	Mean particle diameter (nm) ± S.D.	p
First	BSA concentration (mg/ml)	150	689 ± 41.90	0.033
		250	614 ± 18.52	*
		350	622 ± 17.78	
Second	High-speed emulsification time (min)	8	612 ± 10.54	0.001
		5	621 ± 15.72	**
		2	744 ± 35.59	
Third	Aqueous-to-non-aqueous phase volume ratio (v/v)	0.5:50	599 ± 27.71	0.000
		1:50	613 ± 25.63	**
			945 ± 34.51	
		2:50		
Fourth	Emulsion drop rate (day/min)	10 ± 5	694 ± 24.56	0.035
		30 ± 5	640 ± 36.76	*
		50 ± 5	617 ± 18.08	
Fifth	Heat stabilization temperature (°C)	120 ± 5	722 ± 31.10	0.001
		140 ± 5	585 ± 19.67	**
		160 ± 5	571 ± 26.21	
Sixth	Heat stabilization time (min)	10	610 ± 31.76	0.497
		20	602 ± 17.44	
		30	627 ± 23.52	

* Significant difference at the 95% level of confidence.
** Significant difference at the 99% level of confidence.

particle size, with the lowest phase volume ratio (0.5:50) producing the smallest particle size. At the 2:50 level, the nanoparticles was obtained with wider particle size distribution, however, in the 1:50 phase volume ratio batch, the nanoparticles showed small particle size and good recovery.

The effect of the heat stabilization temperature on nanoparticle size was probably due to the rate and extent of water evaporation from the internal phase. The heat stabilization temperature of 120 °C produced the largest mean particle size indicating that water may still be trapped in the BSA matrix (see Table 1). The higher temperature of heat stabilization provided small particle size of nanoparticles.

With regard of other variables, higher emulsion drop rate leaded to smaller particle size, however, heat stabilization time took little effect on particle size.

The zeta potential of the nanoparticles produced by optimal formulation and technique was −19.3 ± 0.6 Hz, which indicated a stable property.

3.3. The form of HCPT in nanoparticles

3.3.1. The mechanism of HCPT forms transformation

In this research, although HCPT was dissolved in NaOH solution with the carboxylate form at the beginning, the percentage of lactone form of HCPT in resultant BSA nanoparticles could be improved over 95%. During the preparation, HCPT transformed from lactone to carboxylate and finally back to lactone form successfully. The mechanism was explained as follow:

(1) HCPT transformed into carboxylate form when dissolving in NaOH solution.

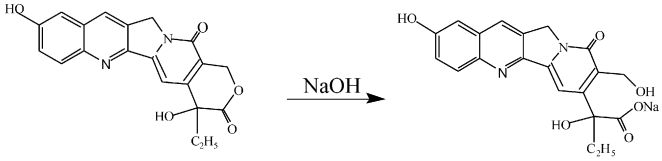

Lactone form Carboxylate form

(2) When aqueous solution was added to castor oil to form w/o emulsion, the saponification reaction occurred between NaOH and castor oil.

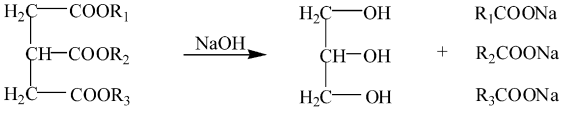

Castor oil

R_1, R_2: Castor acid. R_3: Oleic acid.

(3) Stirring time after high-speed emulsification was prolonged to make sure that the saponification reaction could carried completely. Since NaOH was depleted, the pH value of aqueous phase depressed. HCPT finally transformed back to lactone form.

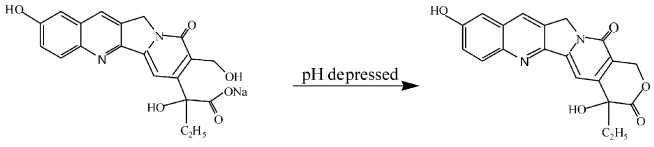

Carboxylate form Lactone form

3.3.2. Effects of some main factors on the form of HCPT

Comparing with the initial method, NaOH solution was applied as water phase to dissolve HCPT and the stirring time

Table 2
The effects of concentration of NaOH and stirring time after high-speed emulsification on the percentage of lactone form

Numbers	Concentration of NaOH (mol/l)	Stirring time after high-speed emulsification (min)	Percentage of lactone form (%)
1	0.04	10	89
2	0.04	30	97
3	0.04	60	98
4	0.07	10	72
5	0.07	30	94
6	0.07	60	97
7	0.1	10	56
8	0.1	30	79
9	0.1	60	83

after high-speed emulsification was prolonged to transform carboxylate form of HCPT into active lactone form. In this test, 90% was considered to be the lowest allowable percentage of lactone form of HCPT.

The concentration of NaOH solution and the stirring time after high-speed emulsification were obviously influenced the percentage of lactone form of HCPT in resultant BSA nanoparticles (showed in Table 2): if the concentration of NaOH solution in formulation was fixed, the percentage of lactone form decreased when the stirring time after high-speed emulsification became shorter. Furthermore, when the concentration of NaOH solution was overmuch than 0.1 mol/l, the nanoparticles could not achieve the required standard of percentage of lactone form, expressing the concentration of NaOH solution in formulation took important effect on the form of HCPT.

According to Table 2, 3-dimensional (3D) contour plot was obtained to describe the effects of concentration of NaOH solution and stirring time on the percentage of lactone form of HCPT, which could also be used for selecting the optimal formulation and technique. All the spots inside the region with red color in Fig. 2 represented that nanoparticles contained higher percentage of lactone form of HCPT under given content values of concentration of NaOH solution and stirring time. Since it's difficult to dissolve 6 mg HCPT in 0.6 ml NaOH solution with the concentration of lower than 0.04 mol/l, the concentration of 0.04 mol/l or higher, which was involved in the region mentioned above, can be pointed out. In our test, the selected point was corresponded with 0.04 mol/l NaOH solution and 40 min of stirring, which was also chosen to be the ultimate optimum formulation and technique.

The reason why the two factors mainly influenced the percentage of lactone form of HCPT was considered that with the sufficient stirring after high-speed emulsification, the saponification reaction could carried out completely, so that the form of HCPT gradually changed from carboxylate to lactone. However, NaOH solution with the higher concentration couldn't completely participate in saponification reaction due to the limited reactive space. Therefore, the pH value was still higher than desired and part of HCPT remained as its carboxylate form.

3.4. Morphology of HCPT–BSA nanoparticles

To investigate the morphology of prepared nanoparticles, light microscope observations were conducted. Fig. 3 shows the light microscope micrograph of the HCPT loaded nanoparticles. It can be seen that all these nanoparticles had a near-spherical shape, and they were dispersed in medium without conglutination.

3.5. Drug loading content, encapsulation efficiency and yield of HCPT–BSA nanoparticles

Several factors may affect drug loading content and drug encapsulation efficiency of the BSA nanoparticles: (1) the affinity of the loaded drug with BSA; (2) drug solubility in water; (3) drug/BSA feeding ratio. Among them, drug/BSA feeding ratio is considered to be the overriding factor in our test.

Fig. 4 displays drug encapsulation efficiency and drug loading content as functions of feeding drug/BSA ratio. The encapsulation efficiency dropped from 70% to 30% with the increase

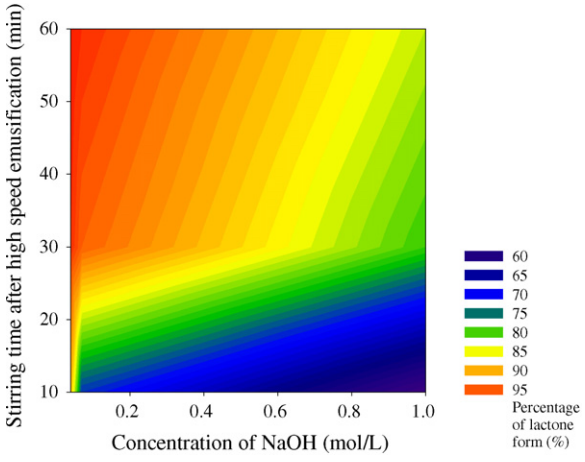

Fig. 2. 3D Contour Plot to describe the effects of concentration of NaOH and stirring time after high-speed emulsification on the percentage of lactone form.

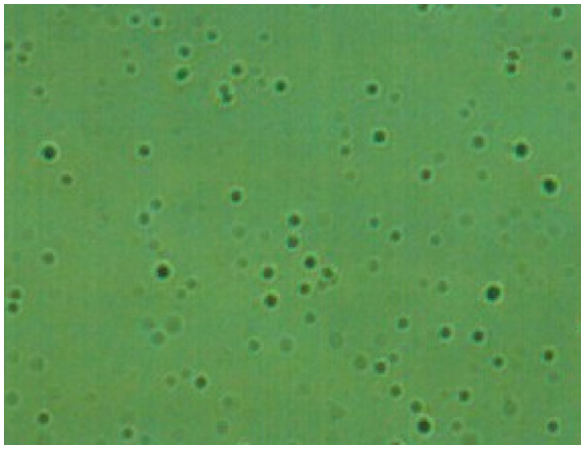

Fig. 3. Light microscope micrographs of BSA nanoparticles prepared by optimal method (magnification = 1500×).

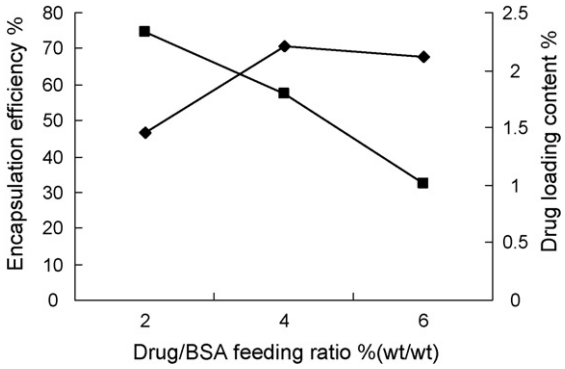

Fig. 4. Drug encapsulation efficiency and drug loading content of the HCPT–BSA nanoparticles as functions of the feeding drug/BSA ratio. BSA concentration was fixed at 250 mg/ml. (■) Encapsulation efficiency; (♦) drug loading content.

of feeding drug/BSA ratio from 2% to 6% (w/w). This may arise from a possible interaction between BSA and HCPT, which can protect HCPT from oil phase and prevent HCPT diffusion towards to oil phase. The encapsulation efficiency was decreased suggesting that the quantity of BSA present becomes insufficient to entrap the total amount of HCPT. In addition, it was found that drug/copolymer feeding ratio higher than 6% (w/w) caused a large amount of particle conglutination and very low nanoparticle yield (less than 40%), implying that the feeding drug whose amount is much higher than its saturation solubility in the polymer matrix may act as a coagulant in the system and hamper the overall stability of the formed nanoparticles.

The curves in Fig. 4 also show the dependence of drug loading content on the drug/BSA feeding ratio. It is clear that nanoparticles with drug/BSA feeding ratios of 4% and 6% have better drug loading content. Considering that the similar drug loading contents were obtained by different drug/BSA feeding ratios of 4% and 6%, we think that HCPT was saturated in BSA when the proportion was beyond 4%. Besides, the increased concentration of HCPT would bring larger particle size and dissatisfactory stability.

The drug loading content, encapsulation efficiency and yield of HCPT–BSA nanoparticles produced by optimal formulation and technique were 2.21%, 57.5% and 90.5%, respectively.

3.6. HCPT release from albumin nanoparticles

Fig. 5 shows that the release of HCPT from HCPT–BSA nanoparticles in pH 7.4 PBS at 37 °C was very slow. After 40 h only about 18% lactone form and 5% carboxylate form of loaded drug were released from the nanoparticles. Then the summation of the two forms of HCPT didn't increase any more, and part of the lactone form of HCPT transformed into carboxylate form gradually. The mechanism of drug release from albumin nanoparticle is dependent on the location of the drug in the carrier as well as on the properties of the nanoparticle matrix (Gupta et al., 1986). Drug can be associated with albumin nanoparticles by either adsorption onto the particle surface or inclusion in the nanoparticle matrix. The release of drug from the particle surface can be achieved by drug dissolution or by drug desorption,

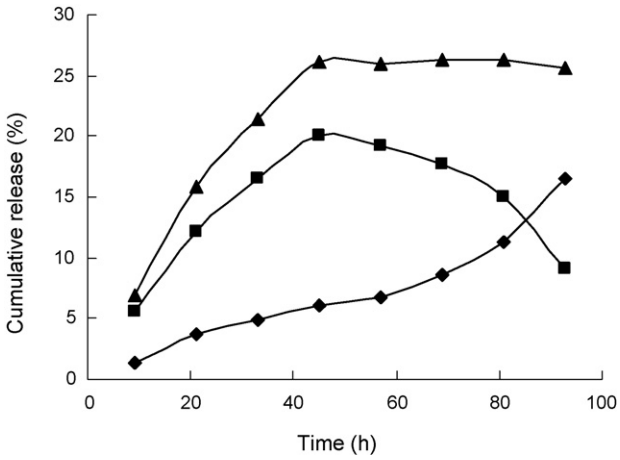

Fig. 5. Drug release behavior of HCPT–BSA nanoparticlesin pH 7.4 PBS. (■) Lactone form of HCPT; (♦) carboxylate form of HCPT; (▲) the summation of lactone and carboxylate forms of HCPT.

so HCPT released slowly due to its poor solubility in pH 7.4 PBS. Provided the albumin matrix of the nanoparticle is stable during in vitro dissolution (it was reasonable owing to the insolubility of denatured BSA), the release of HCPT entrapped within the nanoparticle appears more difficult. Accordingly, the cumulative release of HCPT could only achieve 25%.

According to USP28, trypsin of 750 U/ml was added to pH 7.4 PBS to simulate the condition in vivo. The results of the curve fitting indicated that the drug release from the albumin nanoparticles in the presence of trypsin could be described as an erosion sphere model (Heison and Crowell cube-root equation) (Su et al., 1994; Vergnaud, 1993). Since BSA could be decomposed by tripsin, the release of HCPT obviously quickened, and HCPT located in any possible sites of the microspheres could successfully release. Therefore, in Fig. 6, the cumulative release of HCPT reached more than 90% in 20 h. After that, the summation of the two forms of HCPT changed slightly, and the amount of lactone form decreased while the carboxylate form increased, which was consistent with Fig. 5.

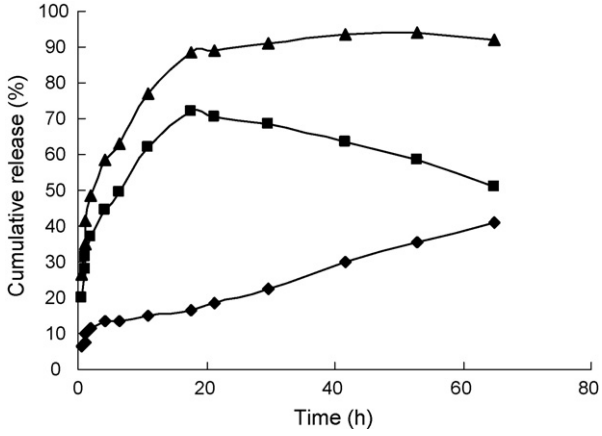

Fig. 6. Drug release behavior of HCPT–BSA nanoparticles in pH 7.4 PBS containing 750 U/ml trypsin. (■) Lactone form of HCPT; (♦) carboxylate form of HCPT; (▲) the summation of lactone and carboxylate forms of HCPT.

3.7. Body distribution in rats of HCPT loaded in nanoparticles

Fig. 7 shows the typical HPLC chromatograms obtained in biodistribution study. It can be seen that under the selected HPLC conditions, HPLC provides good separation between HCPT and the lipophilic substances in tissue homogenates. It shows that the concentration of carboxylate form of HCPT was much lower than that of its lactone form in the investigated organs, which obviously increased the stability of lactone HCPT comparing

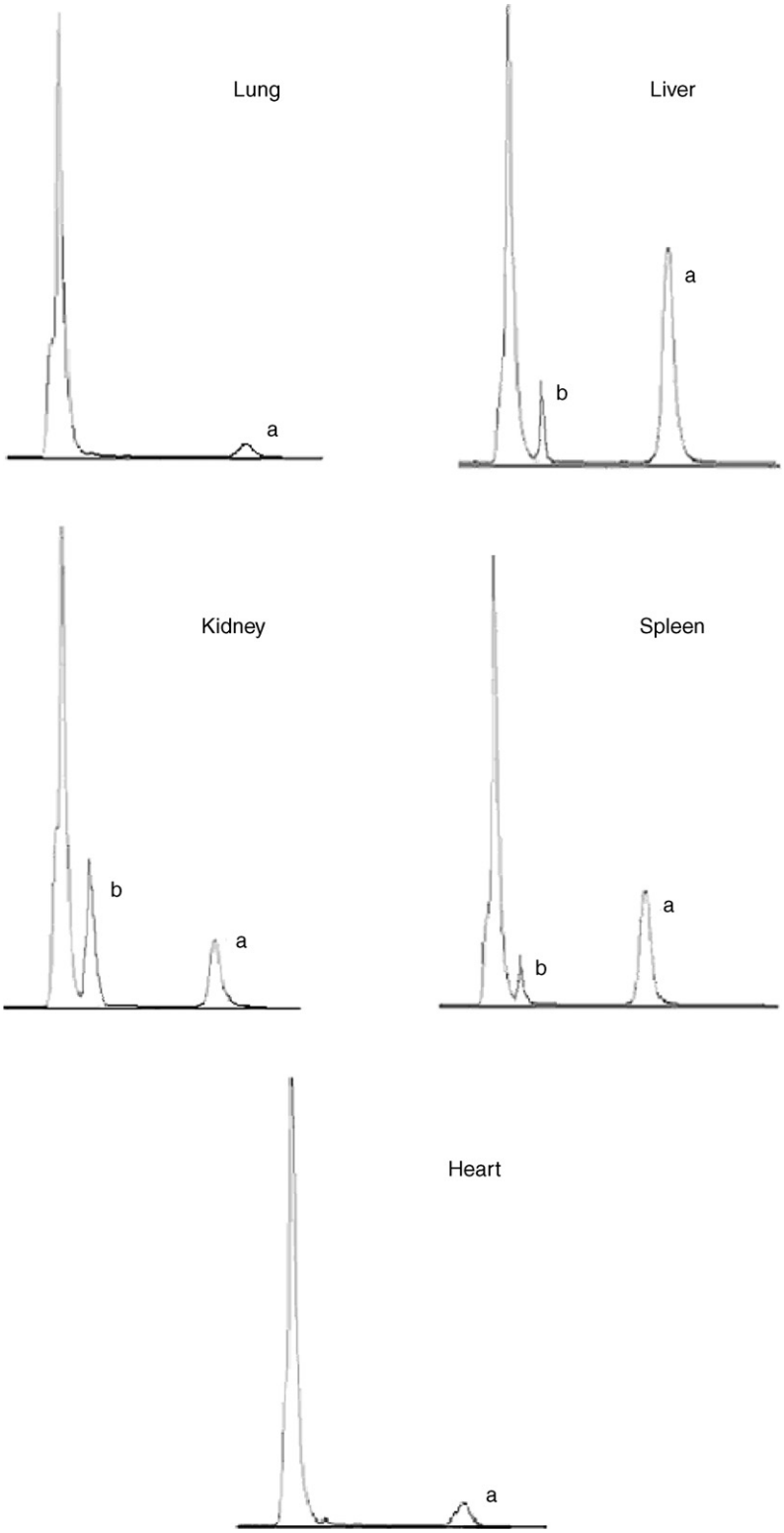

Fig. 7. HPLC analysis of HCPT in rat liver, lung, kidney, spleen and heart. Samples were obtained from rats 4 h after i.v. administration of HCPT at a dose of 5 mg/kg. Peak a: lactone form; peak b: carboxylate form.

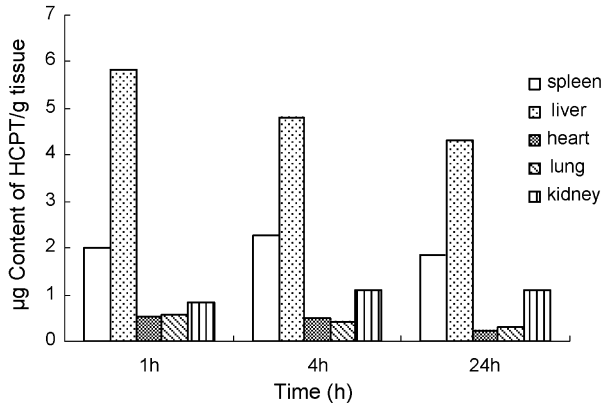

Fig. 8. Body distribution of lactone form of HCPT after i.v. administration of HCPT–BSA nanoparticles in rats.

with the results of i.v. administration of HCPT–DMSO solution (Li and Zhang, 1996), because it was reported that the concentration of lactone HCPT was lower than carboxylate HCPT in liver and kidney. We considered that BSA could effectively retard the HCPT lactone ring opening during the process of drug distribution.

The concentration of HCPT found in sampled tissues at each sampling point was expressed in the content of lactone form of HCPT per gram tissue (see Fig. 8). It is found that the concentration of HCPT in liver and spleen remained relatively high even at 24 h post-injection possibly due to the passive targeting ability of BSA nanoparticles for RES organ. HCPT concentration in kidney, one of the major elimination pathways of the original HCPT, was low. However, the HCPT concentration in lung was even lower, which indicated that the filtration effect of the lung capillary bed didn't work. In addition, the HCPT concentration in heart was lower, too.

The maximum concentration in the liver, 5.3% of the injected dose, was observed at 1 h. At 4 h the drug content in the liver was 4.4%, at 24 h 3.7% of the injected dose. 59.6%, 52.9% and 55.3% of the examined amount in the five organs of lactone HCPT accumulated in livers at 1, 4, and 24 h after injection, respectively. All the datum above showed the liver targeting potential of HCPT–BSA nanoparticles. It was reported in previous research (Sun et al., 2004) that HCPT alkaline solution distributed in tissues of rats, which showed that the concentration of drug in tissues decreased rapidly for the first 4 h. Compared with this our HCPT–BSA nanoparticles exhibited a sustained and steady release in vivo. The body distribution investigation conducted here is preliminary. It could be altered in some degree through the adjustment in particle size. Therefore, more detailed in vivo study on this novel HCPT delivery system is currently under further investigation.

4. Conclusions

HCPT–BSA nanoparticles were prepared by an improved emulsion-heat stabilization technique in this test. Since, HCPT was hardly dissolve in both aqueous and oil phases, the characteristic of high solubility in alkali solution of HCPT was utilized during the preparation process. The percentage of lactone form of HCPT in resultant BSA nanoparticles could be improve over 95% through adjusting the concentration of NaOH solution and the stirring time after high-speed emulsification. And a number of variables, which might affect the final nanoparticle size were investigated to optimize the formulation and technique.

The release of HCPT from the nanoparticles in pH 7.4 PBS at 37 °C was very slowly, however, it was dramatically accelerated in the presence of trypsin. The body distribution showed the liver targeting potential of HCPT–BSA nanoparticles, and this drug delivery system could effectively prevent HCPT from changing into carboxylate form in vivo.

References

Eberth, K., Merry, J., 1983. A comparative study of emulsions prepared by ultrasound and by a conventional method droplet size measurements by means of a coulter counter and microscopy. Int. J. Pharm. 14, 349–353.

Fassberg, J., Stella, V.J., 1992. A kinetic and mechanistic study of the hydrolysis of camptothecin and some analogues. J. Pharm. Sci. 81, 676–684.

Gallo, J.M., Hung, C.T., Perrier, D.G., 1984. Analysis of albumin microsphere preparation. Int. J. Pharm. 22, 63–74.

Gupta, P.K., Hung, C.T., Perrier, D.G., 1986. Albumin microspheres. I. Release characteristics of adriamycin. Int. J. Pharm. 33, 137–146.

Hatefi, A., Amsden, B., 2002. Camptothecin delivery methods. Pharm. Res. 19, 1389–1399.

Jaxel, C., Kohn, K.W., Wani, M.C., 1989. Structure-activity study of the actions of camptothecin derivatives on mammalian topoisomerase. I. Evidence for a specific receptor site and for a relation to antitumor activity. Cancer Res. 49, 1465–1469.

Li, M.K., Folger, H.S., 1979. Acoustic emulsification. Part 2. Breakup of the large primary oil droplets in a water medium. J. Fluid Mech. 88, 513–528.

Li, Y.F., Zhang, R.W., 1996. Reversed-phase high-performance liquid chromatography method for the simultaneous quantitation of the lactone and carboxylate forms of the novel natural product anticancer agent 10-hydroxycamptothecin in biological fluids and tissues. J. Chromatogr. B 686, 257–265.

Lundberg, B.B., 1998. Biologically active camptothecin derivatives for incorporation into liposome bilayers and lipid emulsions. Anti-Cancer Drug Des. 13, 453–461.

Ma, J., Liu, C.L., Zhu, P.L., Jia, Z.P., Xu, L.T., Wang, R., 2002. Simultaneous determination of the carboxylate and lactone forms of 10-hydroxycamptothecin in human serum by restricted-access media high-performance liquid chromatography. J. Chromatogr. B 772, 197–204.

O'Leary, J., Muggia, F.M., 1998. Camptothecins: a review of their development and schedules of administration. Eur. J. Cancer 34, 1500–1508.

Opanasopit, P., Yokoyama, M., Watanabe, M., 2004. Block copolymer design for camptothecin incorporation into polymeric micelles for passive tumor targeting. Pharm Res. 21, 2001–2008.

Opanasopit, P., Yokoyama, M., Watanabe, M., Kawano, K., Maitani, Y., Okano, T., 2005. Influence of serum and albumins from different species on stability of camptothecin-loaded micelles. J. Control. Rel. 104, 313–321.

Rothenberg, M.L., 1997. Topoisomerase I inhibitors: review and update. Ann. Oncol. 8, 837–855.

Sahin, S., Selek, H., Ponche, G., Ercan, M.T., Sargon, M., Hincal, A.A., Kas, H.S., 2002. Preparation, characterization and in vivo distribution of terbutaline sulfate loaded albumin microspheres. J. Control. Rel. 82, 345–358.

Shenderova, A., Burke, T.G., Schwendeman, S.P., 1997. Stabilization of 10-Hydroxycamptothecin in poly (lactide-co-glycolide) delivery vehicles. Pharm. Res. 14, 1406–1413.

Su, X.Y., Al-Kassas, R., Li, A.W.P., 1994. Statistical modeling of ibuprofen release from spherical lipophilic matrices. Eur. J. Pharm. Biopharm. 40, 73–76.

Sun, J.X., Wang, L.N., Yin, L., Zhang, Z.X., 2004. Determination of 10-hydroxycamptothecin in tissues of rats by HPLC-FD. J. China Pharm. Univ. 35, 540–544.

Vergnaud, J.M., 1993. Drug delivery from dosage forms consisting of a drug dispersed in an erodible polymer. In: Controlled Drug Release of Oral Dosage Forms. Ellis Horwood, Chichester, pp. 313–327.

Zhang, Z.R., Lu, W., 1997. Study on liver targeting and sustained release hydroxycamptothecin polybutylcyanoacrylate nanoparticles. Acta Pharm. Sinica 32, 222–227.

Zhang, L.Y., Hua, Y., Jiang, X.Q., 2004. Camptothecin derivative-loaded poly(caprolactone-co-lactide)-b-PEG-b-poly(caprolactone-co-lactide) nanoparticles and their biodistribution in mice. J. Control. Rel. 96, 135–148.